Clin Exp Metastasis
DOI 10.1007/s10585-015-9695-4

RESEARCH PAPER

Epigenetic variations in breast cancer progression to lymph node metastasis

Guillermo Urrutia · Sergio Laurito · Diego M. Marzese · Francisco Gago · Javier Orozco · Olga Tello · Teresita Branham · Emanuel M. Campoy · María Roqué

Received: 13 August 2014 / Accepted: 13 January 2015

Abstract Breast cancer is a heterogeneous disease characterized by the accumulation of genetic and epigenetic alterations that contribute to the development of regional and distant metastases. Lymph node metastasis (LNM) status is the single most important prognostic factor. Metastatic cancer cells share common molecular alterations with those of the primary tumor, but in addition, they develop distinct changes that allow the cancer to progress. There is an urgent need for molecular studies which focus on identifying genomic and epigenomic markers that can predict the progression to metastasis. The objective of this study was to identify epigenetic similarities and differences between paired primary breast tumor (PBT) and LNM. We employed Methylation-Specific-MLPA (Multiplex ligation-dependent probe amplification) to assess the methylation status of 33 cancer-related genes in a cohort of 50 paired PBT and LNM specimens. We found that the methylation index, which represents the degree of aberrantly methylated genes in a specimen, was maintained during the progression to LNM. However, some genes presented differential methylation profiles. Interestingly, *PAX6* presented a significant negative correlation between paired PBT and LNM ($p = 0.03$), which indicated a switch from methylated to unmethylated status in the progression from PBT to LNM. We further identified that the methylation status of *PAX6* on the identified CpG site functionally affected the expression of *PAX6* at the mRNA level. Our study unraveled significant epigenetic changes during the progression from PBT to LNM, which may contribute to improved prognosis, prediction and therapeutic management of metastatic breast cancer patients.

Keywords Breast cancer · Lymph node metastasis · *PAX6* · DNA methylation

Abbreviations

PBT	Primary breast tumor
LNM	Lymph node metastasis
MS-MLPA	Methyl-specific multiplex ligation-dependent probe amplification
PAX6	Paired box 6
CTC	Circulating tumor cells
IHQ	Immunohistochemistry
ER	Estrogen receptor
PR	Progesterone receptor
HER2	Human epidermal growth factor receptor 2
MI	Methylation index
MD	Methylation differences

Introduction

According to the International Agency for Research on Cancer (IARC), breast cancer is the second most common

G. Urrutia · S. Laurito · T. Branham · E. M. Campoy · M. Roqué (✉)
IHEM-CCT-CONICET Mendoza and National University of Cuyo, Mendoza, Argentina
e-mail: mroque@mendoza-conicet.gob.ar

D. M. Marzese
John Wayne Cancer Institute, Providence Saint John's Health Center, Santa Monica, USA

F. Gago · J. Orozco
Medical School of the National University of Cuyo, Mendoza, Argentina

O. Tello
School of Dentistry of the National University of Cuyo, Mendoza, Argentina

Published online: 28 January 2015

cancer in the world and, by far, the most frequent cancer among women with an estimated 1.67 million new cancer cases diagnosed in 2012 (25 % of all cancers) [1]. It is well known that breast cancer is a heterogeneous disease that is classified in molecular subtypes associated with distinct clinical-pathological features. Some of these pathological characteristics have prognostic significance, among which lymph node metastasis (LNM) is the single most important clinical parameter. Patients with lymph LNM have an increased risk of recurrence as evidenced by the shorter five-year disease-free survival [2].

Even though there is a multitude of different cancer types, it has been proposed that all of them share similar characteristics. According to Hanahan and Weinberg [3], these features can be summarized in eight "hallmarks", among which *Invasion and Metastasis* is one of them. This is a key hallmark of malignant tumors, which is acquired during the tumorigenesis by the accumulation of genetic and epigenetic alterations. *Invasion and Metastasis* allows tumors to disseminate, through lymphatic or blood vessels, to colonize and to growth in regional and distant organs. It is known that dissemination of tumor cells is an early event in breast cancer [4]. Circulating tumor cells (CTC) and circulating tumor-free DNA are described in different types of cancers, including breast carcinomas [5]. However, not all disseminated cells have the capacity to anchor and to adapt to an unknown environment. Therefore, it is important to remark that even though invasion is a required step for dissemination, the metastasis success depends on the acquisition of novel genetic and epigenetic alterations that allow the cells to adapt to a different niche.

The importance of aberrant DNA methylation of cancer-related genes has been demonstrated in different carcinogenic processes [6]. These include genes involved in DNA repair and cell cycle regulation [7], angiogenesis [8], and apoptosis [9] among other processes. The epigenomic analyses of tumors that developed into metastasis have identified several novel prognosis markers that can contribute to the improvement of clinical management of metastatic breast cancer patients [10, 11].

Our previous studies revealed that among 46 CpG sites in promoters of cancer-related genes, the aberrant methylation of *RARB* in the PBT was associated with an increased risk for metastasis in regional lymph nodes [12]. This study agreed with evidence from other authors [13] and postulates *RARB* is an important epigenetic marker to predict LNM. Even though different studies have identified valuable markers for PBT, epigenomic alterations of metastatic lesions are still poorly understood.

It has been assumed for several years that the molecular alterations of the PBT are present in secondary lesions. Consequently, this has been the foundation for treating the systemic disease based on proteomic and genomic alterations identified in the PBT, i.e. estrogen receptor (ER), progesterone receptor (PR) and HER2 receptor alterations. However, discordance in gene expression profiles between primary and metastatic tumors have been recently reported [14–16]. An explanation for this discrepancy is the molecular heterogeneity of human tumors [14, 17]. This model suggests that successful CTCs, those that metastasize to regional or distant organs, have alternative molecular alterations compared to those present in the primary tumor. Meanwhile, an alternative hypothesis exists, based on the fact that the metastatic environment differs from the primary tumor environment, and therefore different genetic/epigenetic changes can be acquired in the new colonized niche.

Given that epigenetic modifications are highly dynamic, in contrast with genetic variations, we hypothesized that variations in DNA methylation may help to explain the discordance between PBT and LNM. In this study, we investigated the methylation profile of 33 cancer-related genes in a clinically well-annotated cohort of 25 PBT and paired LNM. Our aim was to identify genes with significant DNA methylation variation that could contribute to a LNM-specific methylation profile.

Materials and methods

Patients

A total of 25 breast cancer patients with PBT and LNM were included in this study (Table 1). All the patients signed an informed consent based on the scientific and ethical principles of the World Medical Associatioń s Declaration of Helsinki. Ethical approval for the study and informed consent was obtained from the Ethics Committee of the School of Medical Sciences, from the National University of Cuyo, Mendoza, Argentina. The surgeries, anatomo-pathological analysis, the treatment and surveillance were performed by the same group of medical doctors involved in the study.

Histopathological analysis

All PBT and their respective LNM were analyzed by the same pathologist (O.T.). Lymph nodes were evaluated by intra-operatory biopsy and posterior hematoxilin and eosin staining to identify the presence and extent of metastasis. Only macrometastasis >2 mm were included in the study. The ER, PR, and epidermal growth factor receptor (HER2) status were analyzed in the PBT specimen by standard immunohistochemistry (IHC). For cases with intermediate IHC results for HER2, fluorescent in situ hybridization was employed to evaluate HER2 gene amplification.

Table 1 Clinical-pathological features of patients

Total patients	25
Primary tumor type	
IDC	21
ILC	3
DCIS	1
Primary tumor side	
Right	5
Left	17
NA	3
Stage	
II	12
III	10
NA	3
Primary tumor grade	
I	3
II	8
III	11
NA	3
Primary tumor biomarkers	
ER	
Positive	14
Negative	8
PR	
Positive	14
Negative	8
HER2	
Positive	3
Negative	19
NA	3

Tumor type, side, stage, grade and membrane biomarkers frequencies are detailed

IDC invasive ductal breast carcinoma, *ILC* invasive lobular carcinoma, *DCIS* in situ ductal carcinoma, *ER* estrogen receptor, *PR* progesterone receptor, *HER2* epidermal growth factor receptor 2

DNA extraction

Tissues were frozen at −80 °C and broken with a frozen mortar. The homogenate was collected and suspended in T_{10} E buffer (10 Mm Tris/HCL and 1 mM EDTA). All samples were incubates for at least during 24 h at −20 °C to improve efficiency of the process. DNA extraction was performed as we previously described [18]. Briefly, homogenate from tumor tissues was dissolved in 3 ml of CTAB solution (2 g/l CTAB (Sigma Aldrich, Bavaria Germany), 100 mM Tris/HCL, 20 mM EDTA and 2 % 2-mercaptoethanol) and incubated at 60 °C during 4 h for membrane lysis. Once the pellet was dissolved, 3 ml of chloroform-isoamylic solution (24:1) was added, mixed during 5 min, and centrifuged at 3,000 rpm for 5 min. Aqueous phase was collected into a new tube and mixed with 9 ml ice-cold 100 % ethanol. Precipitated DNA was dissolved in T_{10}E buffer and stored at −20 °C.

Methylation-specific multiplex ligation-dependent probe amplification (MS-MLPA) assay

In order to assess the methylation status of 46 CpG sites within 33 cancer-related genes (Table 2), the MS-MLPA kits ME001B and ME002 were used. The MS-MLPA reactions were performed according to the manufactureŕs recommendations (MRC Holland, Amsterdam, The Netherlands) introducing subtle modifications (i.e., extended restriction enzyme incubation time and separated ligation and restriction steps) to avoid background signals as we previously reported [18]. The fluorescent-labeled PCR products were separated by capillary electrophoresis in an ABI-3130 sequencer (Applied Biosystems, Foster City, CA, USA) and analyzed by GeneMarker v1.75 software (Softgenetics, State College, PA, USA). This analysis normalizes the data by dividing the peak area of a single probe by the peak areas of control probes. Then the normalized peaks from the analyzed samples are compared to the normalized peaks from the control reaction. A CpG site was considered to be methylated when the methylation dosage ratio was superior to the cut-off threshold of 15 % [7]. DNA methylation level was dichotomized in unmethylated and methylated. Methylation analysis was performed on paired PBT and LNM samples that correspond to the same patients.

Real time polymerase chain reaction

RNA was extracted from PBT and LNM with Trizol Reagent (Life Technologies, USA). 5 µg of total RNA was used for first strand synthesis of cDNA by using M-MLV retro-transcriptase (Promega, USA) and Random Hexamers (Roche, USA) primers. The retro-transcription was carried out during 60 min at 37 °C according to manufactureŕs instructions. One hundred ng of cDNA were used to perform Real-Time PCR using specific primers for *PAX6* and *GAPDH* genes in a RotorGene 6000 thermocycler (Corbett Research, USA). The primers for *PAX6* gene were: forward 5-CTTGGGAAATCCGAGACAGATT-3 and reverse 5-GCTAGCCAGGTTGCGAAGAAC-3; for GAPDH gene: forward 5-TGGACCTGACCTGCCGTCTA-3 and reverse 5-CCCTGTTGCTGTAGCCAAATT-3. Detection of PCR product was carried out using the specific DNA dye EvaGreen (Biotium, USA). The amplification program consisted of 40 cycles of 30 s at 95 °C, 30 s at 60 °C and 30 s at 72 °C, followed by a final melting curve step. The specificity of the PCR products was assessed by melting curve analysis.

Table 2 List of the studied cancer related genes and the CpG sites localization

Gene symbol	Name	CpG site
TIMP3	TIMP metallopeptidase inhibitor 3	172 bp before TSS
APC	Adenomatouspolyposis coli	72 bp to exon 2 (regulatory region)
CDKN2A	Cyclin-dependent kinase inhibitor 2A	997 bp before TSS
CDKN2A	Cyclin-dependent kinase inhibitor 2A	31 bp after TSS
ATM	Ataxia telangiectasia mutated	4,457 bp before TSS
ATM	Ataxia telangiectasia mutated	4,658 bp before TSS
RARB	Retinoic acid receptor beta	651 bp before TSS
RARB	Retinoic acid receptor beta	824bp before TSS
CDKN2B	Cyclin-dependent kinase inhibitor 2B	110 bp before TSS
HIC1	Hypermethylated in cancer 1	1,601 bp before TSS
BRCA1	Breast cancer 1	1,211 bp before TSS
BRCA1	Breast cancer 1	1,321 bp before TSS
CASP8	Caspase 8, apoptosis-relatedcysteinepeptidase	8,560 bp before TSS
CDKN1B	Cyclin-dependent kinase inhibitor 1B	157 bp before TSS
PTEN	Phosphatase and tensinhomolog	1,837 bp before TSS
PTEN	Phosphatase and tensin homolog	1,110 bp before TSS
BRCA2	Breast cancer 2	852 bp before TSS
BRCA2	Breast cancer 2	771 bp before TSS
CD44	CD44 molecule	17 bp before TSS
CD44	CD44 molecule	411 bp before TSS
RASSF1A	Ras association domain family member 1A	141 bp before TSS
RASSF1A	Ras association domain family member 1A	79 bp before TSS
DAPK1	Death-associated protein kinase 1	714 bp before TSS
VHL	Von Hippel-Lindau tumor suppresor	80 bp before TSS
VHL	Von Hippel-Lindau tumor suppresor	34 bp after TSS
ESR1	Estrogen receptor 1	163 bp after TSS
TP73	Tumor protein p73	29,790 bp before TSS
FHIT	Fragile histidine triad	714,220 bp before TSS
CADM1 (IGSF4)	Cell adhesion molecule 1	305 bp before TSS
CADM1 (IGSF4)	Cell adhesion molecule 1	72 bp before TSS
CDH13	Cadherin 13	42 bp before TSS
GSTP1	Glutathione S-transferase pi 1	103 bp after TSS
GSTP1	Glutathione S-transferase pi1	245 bp before TSS
MLH1	MutL homolog 1	382 bp before TSS
TP53	Tumor protein p53	10,905 bp before TSS
PAX5	Paired box 5	661 bp before TSS
TP73	Tumor protein p73	29,551 bp before TSS
WT1	Wilms tumor 1	412 bp before TSS
CHFR	Checkpoint with forkhead ring finger domains	407 bp before TSS
RB1	Retinoblastoma 1	520 bp before TSS
RB1	Retinoblastoma 1	323 bp before TSS
THBS1	Thrombospondin 1	834 bp before TSS
STK11	Serine/threonine kinase 11	425 bp before TSS
PYCARD	PYD and CARD domain containing	190 bp before TSS
PAX6	Paired box 6	49 bp before TSS
GATA5	GATA binding protein 5	658 bp before TSS

Gene names and gene symbols are from the HGNC data base; CpG site location was obtained from the MS-MLPA manufacturer's information and confirmed by CLC SequenceViewer 6 Software

TSS transcription start site, *bp* basepairs

Relative expression normalization of genes of interest was carried out using *GAPDH* gene expression as endogenous reference control by the ddCq method. Cycle Threshold (C_T) and Efficiency (E_{Amp}) values were calculated by means of RotorGene 6000 software v1.7 (Corbett Research, USA). To confirm amplifications, PCR products were resolved on 2 % agarose gels.

Statistical analysis

The normality of the distribution of the methylation index (MI) was assessed by Kolmogorov- Smirnov test. Student's T test was performed to compare MI in PBT and LNM. In order to decrease the influence of unmethylation events by the excess of ceros in the data, only genes that were methylated in more than 10 % of the samples were included for the statistical analyses. The relation between the methylation of CpG sites and tissue (PBT or LNM) was assessed by the Fisher Exact test. To compare differences of methylation in paired samples, the non-parametric Sign Test for nominal variables was applied. All statistical analyses were performed using the software SPSS v17 (SPSS Inc, Chicago, IL, USA), results with p values less than 0.05 were considered statistically significant.

Hierarchical clustering analysis and heat maps were performed using the software MultiExperiment Viewer MeV v4.6 (TM 4 group, Dana Farber Cancer Institute, Boston, MA, USA).

Results

The DNA methylation index is maintained in breast cancer progression from primary tumor to LNM

The methylation profile of 46 CpG sites located in 33 cancer-related genes was analyzed in 25 paired PBT and LNM using a dichotomized criterion (Fig. 1). As controls, methylation analyses on surgery margins and peripheral blood leukocytes were performed. These controls were unmethylated in the 46 studied CpG sites.

The number of aberrantly methylated CpG sites in each sample was defined as the MI. While PBT samples presented a mean MI = 9.8 (SD = 3.82; range 4–20), LNM presented a mean MI = 9.28 (SD = 3.55; range 1–15). No significant differences were detected by comparing the mean MI between both groups (Student's T Test for independent samples; $p = 0.59$; Table 3). This observation suggested that the number of aberrantly methylated regions is maintained during the progression from PBT to LNM.

Differences in methylation profiles of primary breast tumors and paired lymph node metastasis

By comparing the methylation signature within each pair, we observed that most of the analyzed CpG sites maintained the DNA methylation statuses during progression from PBT to LNM. For example, this means that when *CDKN1B* was methylated in the PBT, the same alteration was found in the paired LNM. However, we observed that some CpG sites, e.g. *RARB, DAPK1*or *PAX6,* presented a variation in the methylation frequency between PBT and LNM (Fig. 2).

To identify differences in the epigenetic profiles of paired PBT and LNM samples, we assigned a Methylation difference (MD) value to each of the 46 CpG sites as follows: **0** for "no difference between methylation status of PBT and LNM," **1** for "unmethylated in PBT + methylated in LNM" and **−1** for "methylated in PBT + unmethylated in LNM." Using this approach, each CpG site had a MD value for each sample pair (Fig. 1).

As observed in Fig. 1, most of the MD values were zero, which revealed that most of the methylation statuses are maintained within the pair. To identify whether a CpG site changed in a specific direction (methylation gains or losses), we performed a more detailed analysis by adding the MD values of each CpG site across the paired samples. We identified that 16/46 sites (35 %) presented MD sum = 0, which indicated no variation in the methylation of these CpG sites between PBT and LNM or changes in a stochastic way (some gains, some losses; Fig. 1; e.g. *CDKN2A* and *CDKN2B* genes). Interestingly, 25/46 CpG sites (55 %) presented MD sum values up to +4, which indicated that the methylation of these CpG sites moderately changed during progression to LNM. Remarkably, 5 CpG sites (10 %) presented a relatively high absolute MD sum: 1 CpG site in *PAX6* (MD sum = −7), 2 CpG sites in *RASSF1A* (MD sum = −6), 1 CpG site in *PAX5* (MD sum = −5) and 1 CpG site in *THBS1* (MD sum = + 5; lower row in Fig. 1). The negative values for MD sum in *PAX6, RASSF1A* and *PAX5* indicated that these genes were methylated in the PBT and unmethylated in the respective LNM. On the other hand, the positive value for MD sum in *THBS1* indicated that this gene was unmethylated in the PBT and methylated in LNM. To determine whether these observations were statistically significant, a crosstab analysis using Fisher's Exact Test was performed between tissue sample (PBT or LNM) and methylation status (methylated or unmethylated). In order to decrease the interference of zeros (unmethylated sites), CpG sites methylated in less than 10 % of the samples were excluded. This selection reduced the number of 46 CpG sites to 24, located within 20 cancer-related genes. Significant differences for *PAX6* ($p = 0.046$) and *PAX5* ($p = 0.048$) genes


TIMP3
APC
CDKN2A$_a$
ATM$_a$
RARB$_a$
CDKN2B
HIC1
BRCA1$_a$
CASP8
CDKN1B
PTEN
BRCA2$_a$
Cd44$_a$
RASSF1$_a$
DAPK1
VHL
ESR
RASSF1$_b$
Tp73$_a$
FHIT
IGSF4$_a$
CDH13
GSTP1$_a$
MLH1
BRCA1$_b$
BRCA2$_b$
ATM$_b$
Tp53
PTEN
PAX5
Tp73$_b$
Wt1
VHL
GSTP1$_b$
CHFR
Rb$_a$
THBS1
IGSF4$_b$
STK1
PYCARD
PAX6
CDKN2A$_b$
GATA5
RARB$_b$
Cd44$_b$
Rb$_b$
PBT
SLNM
Pair 1
MD 1
Pair 2
MD 2
Pair 3
MD 3
Pair 4
MD 4
Pair 5
MD 5
Pair 6
MD 6
Pair 7
MD 7
Pair 8
MD 8
Pair 9
MD 9
Pair 10
MD 10
Pair 11
MD 11
Pair 12
MD 12
Pair 13
MD 13
Pair 14
MD 14
Pair 15
MD 15
Pair 16
MD 16
Pair 17
MD 17
Pair 18
MD 18
Pair 19
MD 19
Pair 20
MD 20
Pair 21
MD 21
Pair 22
MD 22
Pair 23
MD 23
Pair 24
MD 24
Pair 25
MD 25
MD sum

◀**Fig. 1** Spreadsheet showing methylation profile of 46 CpG sites in 33 cancer-related genes. Genes are represented in columns and paired samples from the same patients in rows. [a,b] super-index indicate two different CpG sites in a same gene. To establish methylation status, a dichotomized criterion was applied. For each CpG site in each sample, a colored box is used as follows: *red boxes* represent methylated status (1); *green boxes* represent unmethylated status (0). After the two rows showing the primary breast tumor and the lymph node metastasis methylation profile, a third row describes the Methylation Differences values (MD) for that pair. Methylation Difference value −1 indicates methylated in primary breast tumor and unmethylated in lymph node metastasis; Methylation Difference value 1 indicates unmethylated in primary breast tumor and methylated in lymph node metastasis; Methylation Difference value cero indicates no differences between primary breast tumor and lymph node metastasis. At the bottom, a Methylation Difference sum row is calculated by summing the individual Methylation Difference values of each pair for each CpG site. *PAX6* presents the largest negative Methylation Difference sum value (−7). (Color figure online)

Table 3 Methylation index in primary tumors and paired lymph node metastases

Matched PBT–LNM	MI
PBT 1	12
LNM 1	12
PBT 2	20
LNM 2	15
PBT 3	11
LNM 3	11
PBT 4	6
LNM 4	9
PBT 5	6
LNM 5	10
PBT 6	8
LNM 6	11
PBT 7	16
LNM 7	15
PBT 8	10
LNM 8	14
PBT 9	8
LNM 9	8
PBT 10	10
LNM 10	9
PBT 11	5
LNM 11	6
PBT 12	14
LNM 12	9
PBT 13	5
LNM 13	9
PBT 14	12
LNM 14	14
PBT 15	8
LNM 15	9
PBT 16	7
LNM 16	9
PBT 17	12
LNM 17	11
PBT 18	10
LNM 18	11
PBT 19	15
LNM 19	4
PBT 20	11
LNM 20	9
PBT 21	6
LNM 21	4
PBT 22	11
LNM 22	11
PBT 23	4
LNM 23	1
PBT 24	11
LNM 24	7
PBT 25	8
LNM 25	1

PBT primary breast tumor, *LNM* lymph node metastasis

were detected. *THBS1* and *RASSF1A* genes did not present significant differences ($p > 0.05$; Table 4).

In order to detect directional differences in the matched samples, the Sign Test for paired samples was applied. This test confirmed that, even though some CpG sites showed differences among paired PBT and LNM (e.g. *RARB*, *TP73* and *GATA5*), the only two genes which showed a directional change were *PAX5* and *PAX6* (Table 5).

After these observations, it was clear that *PAX6* and *PAX5* genes were contributing to a significant and directional epigenetic difference between PBT and their respective LNM. Most of the PBT, which presented these genes methylated, lost its methylation status in the respective LNM. We subsequently centered our attention on *PAX6*, the CpG site that presented the largest MD sum.

Expression levels of *PAX6* differ between primary breast tumors and matched lymph node metastasis

To functionally evaluate the role of the DNA methylation status on *PAX6* gene expression, Real Time PCR assays were performed to compare *PAX6* expression levels in PBT and LNM. Due to the high genetic and epigenetic heterogeneity of tumors and lymph nodes, we first performed the studies on total RNA extracted from cell lines. Therefore, we included 3 cell lines with extreme values of methylation percentage for *PAX6*, i.e. the human breast cancer cell lines

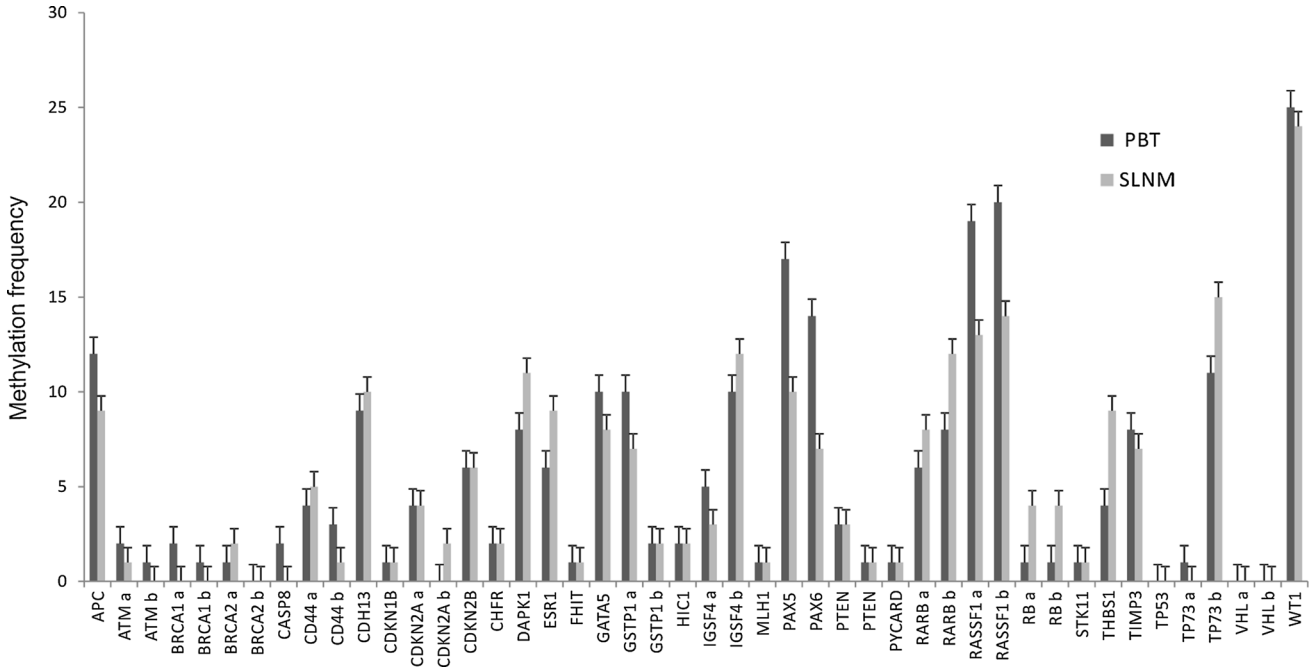

Fig. 2 Histogram showing methylation frequencies of the 46 included CpG sites in primary breast tumors (represented as *dark bars*) and lymph node metastasis (represented as *grey bars*) in alphabetic order. [a,b] super-index indicate two different CpG sites in the promoter or first exon regions in a same gene

Table 4 Crosstab analysis by Fisher Exact test of the methylation status of CpG sites in primary breast tumors and lymph node metastasis

CpG island	P value
PAX6	**0.04**
PAX5	**0.04**
TIMP3	0.76
APC	0.40
CDKN2A	1.00
RARB[a]	0.53
CDKN2B	1.00
PTEN	1.00
CD44	0.72
RASSF1A[a]	0.07
DAPK1	0.39
ESR1	0.36
RASSF1A[b]	0.08
IGSF4	0.45
CDH13	0.77
GSTP1	0.38
TP73	0.26
WT1	0.32
RB1[a]	0.16
THBS1	0.11
IGSF4	0.57
GATA5	0.56
RARB[b]	0.25
RB1[b]	0.16

PAX6 and PAX5 (shown in bold in table) are the only genes which reveal significant difference in lymph node metastasis compared to primary tumors

[a,b] Super−index indicate two different CpG sites in the promoter or first exon regions in a same gene

T47-D and MCF7 with 100 % methylation and the human erythro-leukemia cell line K-562 cell line with 0 % methylation in *PAX6*. Real Time PCR revealed higher expression of PAX6 in cell lines with *PAX6* gene unmethylated (K562) than in cell lines with *PAX6* methylated (T47-D and MCF7; Fig. 3a). Afterwards, Real Time PCR analyses were performed on PBT and LNM with different methylation levels. By comparing the expression of *PAX6* relative to *GAPDH*, we observed that PBTs with high *PAX6* methylation (62 % of the DNA sample) showed a decreased expression compared to PBTs with low *PAX6* methylation (10 % of the DNA sample). In addition, comparisons among LNM with different methylation levels revealed that the expression of *PAX6*in methylated LNM was significantly lower than in unmethylated LNM ($p < 0.05$; Fig. 3a). Our data suggested that the

Table 5 Non-parametric Sign Test analysis comparing differences between PBT and LNM for the methylation status of 24 CpG sites

CpG site	N° pairs	Odd results		Tie results	P value
		Negative differences (methylated in PBT + unmethylated in LNM)	Positive differences (unmethylated in PBT + methylated in LNM)		
PAX6	**25**	**8**	**1**	**16**	**0.03**
PAX5	**25**	**8**	**1**	**16**	**0.03**
TIMP3	**25**	2	1	22	1.00
APC	**25**	4	1	20	0.37
CDKN2A	**25**	1	1	23	1.00
RARB[a]	**25**	2	4	19	0.68
CDKN2B	**25**	2	2	21	1.00
PTEN	**25**	1	1	23	1.00
CD44	**25**	1	2	22	1.00
RASSF1[a]	**25**	7	1	17	0.07
DAPK1	**25**	1	4	20	0.37
ESR1	**25**	0	3	22	0.25
RASSF1[b]	**25**	7	1	17	0.07
IGSF4	**25**	2	0	23	0.5
CDH13	**25**	0	1	24	1.00
GSTP1	**25**	4	1	20	0.37
TP73	**25**	2	6	17	0.28
WT1	**25**	1	0	24	1.00
RB[a]	**25**	1	4	20	0.37
THBS1	**25**	0	5	20	0.06
IGSF4	**25**	1	3	21	0.62
GATA5	**25**	5	3	17	0.72
RARB[b]	**25**	3	7	15	0.34
RB[b]	**25**	0	3	22	0.25

The analysis reveals negative differences (Methylated in PBT + Unmethylated in LNM) for PAX6 and PAX5 (shown in bold in table)

[a,b] Super-index indicate two different CpG sites in the promoter or first exon regions in a same gene

methylation of the CpG site under study has a functional impact on the expression of the*PAX6* gene.

By combining the methylation and expression levels of two LNM and two PBT in a scatter plot, a trend is observed showing a negative correlation between the DNA methylation and the gene expression levels (Fig. 3b).

Discussion

In this study, the methylation profile of 46 CpG sites located in 33 cancer-related genes was analyzed in 25 paired PBT–LNM. Our results revealed no significant differences in the MI between the two groups. This suggested that the magnitude of epigenetic deregulation is maintained through the metastatic process. We identified one CpG site in *PAX6* which presented significant changes in the methylation status during the progression to LNM. This change consisted of a methylation-to-unmethylation switch from PBT to LNM. We also established that this methylation has an impact on the expression of the *PAX6* gene in PBT and in LNM, which revealed that this epigenetic change induces a functional modification in the metastasis.

Many authors have contributed to identifying the important role of aberrant promoter methylation in the metastatic process of breast cancer [19–21]. However, the focus of most of these studies has been centered on detecting molecular alterations in the primary tumors with prognostic value to predict the metastasis development. In previous studies, we found that PBTs with methylated *RARB* were associated with an increased risk for LNM [12]. Interestingly, this observation has been confirmed by other studies using independent patient cohorts [13].

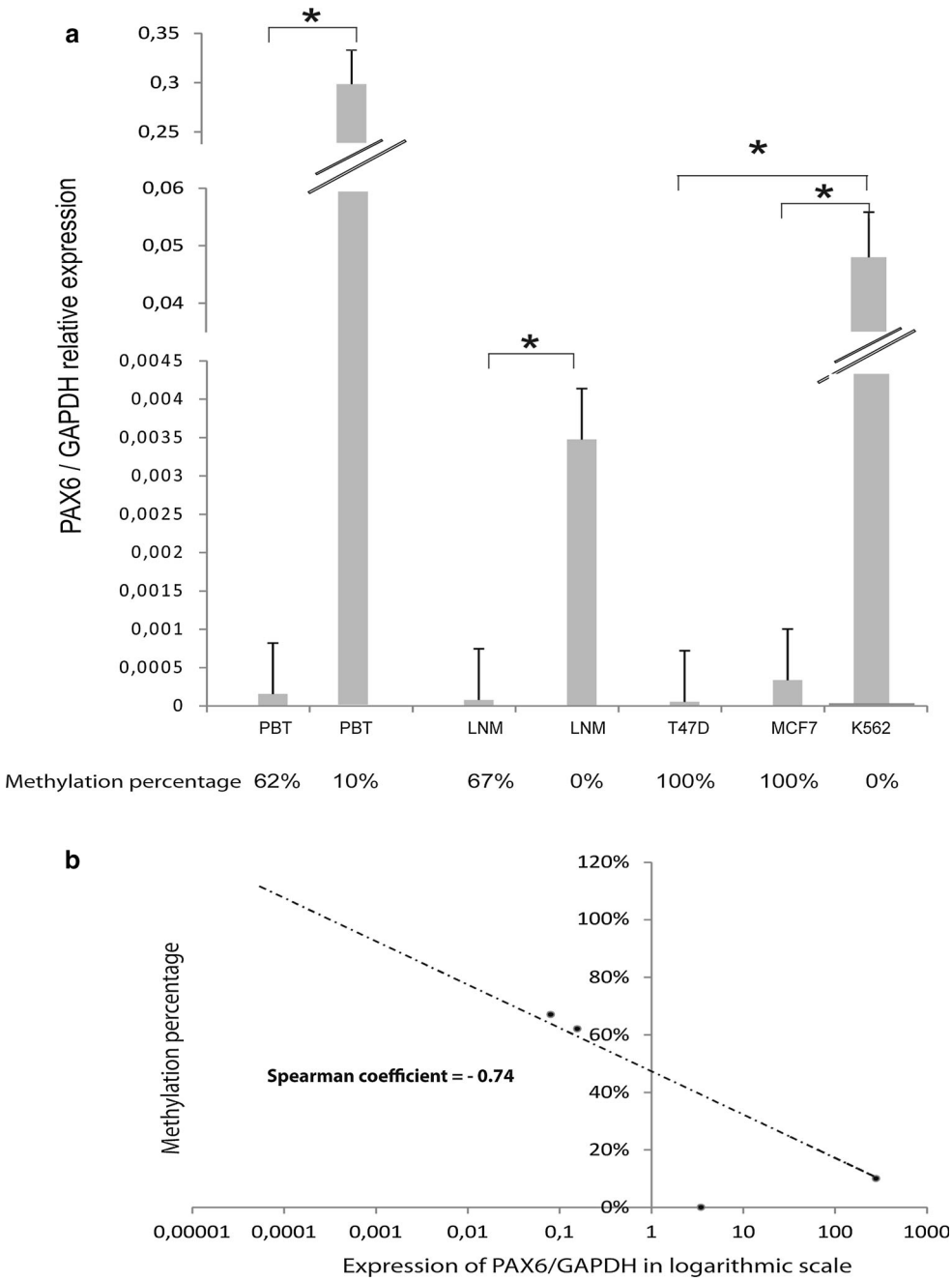

Fig. 3 **a** Relative expression histogram of *PAX6* in different primary breast tumor, lymph node metastasis and cell lines. *Y-axis* represents PAX6/GAPDH relative expression, *X-axis* show primary breast tumor, lymph node metastasis. The methylation percentage is showed below each sample. Significant differences are shown between same sample types with different methylation levels. **b**. Scatter plot showing how higher methylation percentages present lower *PAX6* expression. A dotted-line shows the inverse relation between methylation and expression

However, to date, there is a lack of studies focused on identifying epigenetic alterations occurring in matched PBT–LNM samples.

In contrast with our findings, other authors have reported differences in the number of methylated regions between primary tumors and metastatic tissues using methylation-specific PCR [22] and microarray [23] approaches. These apparently discordant conclusions could be explained by different sets of studied genes, by different methodologies and, most importantly, by the different approach we used when matching samples from the same patient.

The epigenetic variability among paired samples can arise from the primary tumor heterogeneity. In this case, we can speculate that PBT cells *without PAX6* methylation would have the capacity to escape from the breast epithelium and colonize new niches. However, an alternative explanation could be that, since epigenetic modifications are highly dynamic, PBT cells *with PAX6* methylation can escape from the breast epithelial, but when they arrive to the lymph node microenvironment, a selection pressure switches to unmethylated *PAX6* in order to survive in the new niche.

The paired box 6 (*PAX6*) gene was first identified as a member of the murine multigene family with functions in the developmental control in Drosophila [24]. In human cancer, there exists controversial information about *PAX6*. In glioblastomas, it has been postulated as a tumor suppressor gene, whose down-regulation enhances cell invasiveness [25]. In other cancer types, the opposite function of *PAX6* is proposed. Both proliferation and invasion are promoted by *PAX6* in colon cancer [26]. The authors postulate *PAX6* as transcription factor which induces the expression of pro-metastatic proteins MMP2 and MMP9. Moreover, in lung cancer cell lines, the inhibition of *PAX6* inhibits cell proliferation [27], and in retinoblastoma, the overexpression of P*AX6* has been reported [28]. Based on our observations, we support the hypothesis that *PAX6* has a pro-metastatic role in breast cancer, similar to what has been observed by others in colon and lung cancer. We propose that PBT cells *without PAX6* methylation can express the gene, and therefore acquire the capacity to start the epithelial-mesenquimal transition, invade neighbor tissues and escape through the lymphatic or blood vessels to the nearest lymph node.

Due to the requirement to have paired PBT and LNM, one of the major limits of this work is the modest number of patients. To validate the findings of this study and further conclude upon these results, the number of samples should be increased. However, the role of these significant epigenetic differences between PBT and LNM might provide novel biomarkers for screening patients at risk for metastasis, which might improve prognosis and therapeutic management of metastatic breast cancer patients.

Acknowledgments This work was partially funded by the National University of Cuyo, Mendoza, Argentina and the argentine National Cancer Institute. We thank to Nellie Nelson for her critical revision of our manuscript. DMM was supported by the Margie and Robert E. Petersen Foundation.

Conflict of interest The authors declare no conflicts of interest.

References

1. Siegel R, Ma J, Zou Z, Jemal A (2014) Cancer Statistics. J Clin 64:9–29
2. Senkus E, Kyriakides S, Penault-Llorea F, Poortmans P, Thompson A, Zackrisson S, Cardoso F, ESMO Guidelines Working Group (2013) Primary breast cancer: ESMO clinical practice guidelines for diagnosis, treatment and follow up. Ann Oncol 24:7–23
3. Hanahan D, Weinberg RA (2011) Hallmarks of cancer: the next generation. Cel 144:646–674
4. Taback B, Hoon DS (2004) Circulating nucleic acids in plasma and serum: past, present and future. Curr Opin Mol Ther 6: 273–278
5. Rykova EY (2008) Methylation-based analysis of circulating DNA for breast tumor screening. Ann NY Acad Sci 1137(1): 232–235
6. Esteller M, Fraga MF, Guo M, Garcia-Foncillas J, Hedenfalk I, Godwin AK, Trojan J, Vaurs-Barriere C, Bignon YJ, Ramus S, Benitez J, Caldes T, Akiyama Y, Yuasa Y, Launonen V, Canal MJ, Rodriguez R, Capella G, Peinado MA, Borg A, Aaltonen LA, Ponder BA, Baylin SB, Herman JG (2001) DNA methylation patterns in hereditary human cancers mimic sporadic tumorigenesis. Hum Mol Genet 10:3001–3007
7. Moelans CB, Verschuur-Maes AH, van Diest PJ (2011) Frequent promoter hypermethylation of BRCA2, CDH13, MSH6, PAX5, PAX6 and WT1 in ductal carcinoma in situ and invasive breast cancer. J Pathol 225:222–231
8. Lindner DJ, Wu Y, Haney R, Jacobs BS, Fruehauf JP, Tuthill R, Borden EC (2013) Thrombospondin-1 expression in melanoma is blocked by methylation and targeted reversal by 5-Aza-deoxycytidine suppresses angiogenesis. Matrix Biol 32:123–132
9. Widschwendter M (2001) Epigenetic downregulation of the retinoic acid receptor-beta2 gene in breast cancer. J Mammary Gland Biol Neoplas 6(2):193–201
10. Bergman Y, Cedar H (2013) DNA methylation dynamics in health and disease. Nat Struct Mol Biol 20:274–281
11. Flanagan JM, Cocciardi S, Waddell N, Johnstone CN, Marsh A, Henderson S, Simpson P, Da Silva L, Khanna K, Lakhani S, Boshoff C, Chenevix-Trench G (2010) DNA methylome of familial breast cancer identifies distinct profiles defined by mutation status. Am J Hum Genet 86:420–433
12. Marzese DM, Hoon DS, Chong KK, Gago FE, Orozco JI, Tello OM, Vargas-Roig LM, Roque M (2012) DNA methylation index and methylation profile of invasive ductal breast tumors. J Mol Diagn 14:613–622
13. Twelves D, Nerurkar A, Osin P, Dexter T, Ward A, Gui GP, Isacke CM (2013) DNA promoter hypermethylation profiles in breast duct fluid. Breast Cancer Res Treat 139:341–350
14. Sighoko D, Liu J, Hou N, Gustafson P, Huo D (2014) Discordance in hormone receptor status among primary, metastatic, and second primary breast cancers: biological difference or misclassification? Oncologist 19:592–601
15. Yao ZX, Lu LJ, Wang RJ, Jin LB, Liu SC, Li HY, Ren GS, Wu KN, Wang DL, Kong LQ (2014) Discordance and clinical significance of ER, PR, and HER2 status between primary breast cancer and synchronous axillary lymph node metastasis. Med Oncol 31:1–7
16. Aurilio G, Disalvatore D, Pruneri G, Bagnardi V, Viale G, Curigliano G, Adamoli L, Munzone E, Sciandivasci A, De Vita F, Goldhirsch A, Nole F (2014) A meta-analysis of oestrogen receptor, progesterone receptor and human epidermal growth factor receptor 2 discordance between primary breast cancer and metastases. Eur J. Cancer 50:277–289
17. Ibrahim T, Farolfi A, Scarpi E, Mercatali L, Medri L, Ricci M, Nanni O, Serra L, Amadori D (2013) Hormonal receptor, human epidermal growth factor receptor-2, and Ki67 discordance between primary breast cancer and paired metastases: clinical impact. Oncology 84:150–157
18. Marzese DM, Gago FE, Vargas-Roig LM, Roque M (2010) Simultaneous analysis of the methylation profile of 26 cancer related regions in invasive breast carcinomas by MS-MLPA and drMS-MLPA. Mol Cell Probes 24:271–280
19. Feng W, Orlandi R, Zhao N, Carcangiu ML, Tagliabue E, Xu J, Bast RC Jr, Yu Y (2010) Tumor suppressor genes are frequently methylated in lymph node metastases of breast cancers. BMC Cancer 10:378
20. Metge BJ, Frost AR, King JA, Dyess DL, Welch DR, Samant RS, Shevde LA (2008) Epigenetic silencing contributes to the loss of

BRMS1 expression in breast cancer. Clin Exp Metastasis 25:753–763
21. Rivenbark AG, Livasy CA, Boyd CE, Keppler D, Coleman WB (2007) Methylation-dependent silencing of CST6 in primary human breast tumors and metastatic lesions. Exp Mol Pathol 83:188–197
22. Alevizos L, Kataki A, Derventzi A, Gomatos I, Loutraris C, Gloustianou G, Manouras A, Konstadoulakis M, Zografos G (2014) Breast cancer nodal metastasis correlates with tumor and lymph node methylation profiles of Caveolin-1 and CXCR4. Clin Exp Metastasis 31:511–520
23. Skryabin NA, Tolmacheva EN, Lebedev IN, Zavyalova MV, Slonimskaya EM, Cherdyntseva NV (2013) Dynamics of aberrant methylation of futional groups of genes in progression of breast. Cancer Mol Biol 47:302–310
24. Walther C, Gruss P (1991) Pax-6, a murine paired box gene, is expressed in the developing CNS. Development 113:1435–1449
25. Huang BS, Luo QZ, Han Y, Li XB, Cao LJ, Wu LX (2013) microRNA-223 promotes the growth and invasion of glioblastoma cells by targeting tumor suppressor PAX6. Oncol Rep 30:2263–2269
26. Li Y, Li Y, Liu Y, Xie P, Li F, Li G (2014) PAX6, a novel target of microRNA-7, promotes cellular proliferation and invasion in human colorectal cancer cells. Dig Dis Sci 59:598–606
27. Zhao X, Yue W, Zhang L, Ma L, Jia W, Qian Z, Zhang C, Wang Y (2014) Downregulation of PAX6 by shRNA inhibits proliferation and cell cycle progression of human non-small cell lung cancer cell lines. PLoS One 9:e85738
28. Wang J, Wang X, Wu G, Hou D, Hu Q (2013) MiR-365b-3p, down-regulated in retinoblastoma, regulates cell cycle progression and apoptosis of human retinoblastoma cells by targeting PAX6. FEBS Lett 587:1779–1786